BEAM-BASED IMPEDANCE MEASUREMENT TECHNIQUES *

V. Smaluk†,
NSLS-II, Brookhaven National Laboratory, USA

Abstract

Characterization of a vacuum chamber impedance is necessary to estimate stability conditions of a particle beam motion, to find a limit of the beam intensity and characteristic times of single-bunch and multi-bunch instabilities. For a new accelerator project, minimization of the impedance is now the mandatory requirement for the vacuum chamber design. For an accelerator in operation, the impedance can be measured experimentally using various beam-based techniques. The beam-impedance interaction manifests itself in measurable beam parameters, such as betatron tunes, closed orbit, growth rates of instabilities, bunch length and synchronous phase. The beam-based techniques developed for measurement of the longitudinal and transverse impedance are discussed, including theoretical basics and experimental results.

WAKE FUNCTIONS AND IMPEDANCES

In a theory of collective effects, the interaction of a particle beam with electromagnetic fields induced by the beam itself is described in terns of wake functions. These electromagnetic fields are called wake fields because they never propagate ahead of a relativistic particle. The wake function is defined as a normalized integral of the Lorentz force that acts on a test particle moving behind a leading particle which excites the wake fields. To analyze the beam stability in most practical cases, it is enough to consider only monopole longitudinal $W_\parallel$ and dipole transverse $\mathbf{W}_\perp$ wake functions. The longitudinal wake function is obtained by integrating the electric field component E_z, which is parallel to the velocity $\mathbf{v}$ ($|\mathbf{v}| = c$) of the particles moving on the same trajectory [1]:

$$W_\parallel(\tau) = -\frac{1}{q}\int_{-\infty}^{\infty} E_z(t,\tau)\,\mathrm{d}t\,, \qquad (1)$$

where q is the charge of leading particle, $\tau = s/c$, s is the distance between the leading and trailing particles, c is the speed of light. The dipole transverse wake function is determined similarly to the longitudinal one as an integral of transverse electromagnetic forces normalized by the dipole moment qr of the leading particle (r is the transverse offset); it is a vector with horizontal and vertical components:

$$\mathbf{W}_\perp(\tau) = -\frac{1}{q\,r}\int_{-\infty}^{\infty} [\mathbf{E}(t,\tau) + \mathbf{v}\times\mathbf{B}(t,\tau)]_\perp\,\mathrm{d}t\,. \qquad (2)$$

The longitudinal and transverse wake functions are related to each other by the Panofsky-Venzel theorem [1, 2].

For a beam with arbitrary charge distribution, its interaction with wake fields is described by the wake potential V, which is a convolution of the wake function W and the longitudinal charge density $\lambda(t)$:

$$V(\tau) = \int_0^{\infty} W(t)\lambda(\tau - t)\mathrm{d}t\,, \qquad (3)$$

where $\lambda(t)$ is normalized as $\int_{-\infty}^{\infty} \lambda(t)\mathrm{d}t = 1$.

In the frequency domain, each part of the vacuum chamber is represented by a frequency-dependent impedance. Longitudinal $Z_\parallel$ and transverse $Z_\perp$ impedances are defined as Fourier transforms of the corresponding wake functions:

$$Z_\parallel(\omega) = \int_{-\infty}^{\infty} W_\parallel(\tau)\, e^{-i\omega\tau}\,\mathrm{d}\tau\,,$$
$$Z_\perp(\omega) = i\int_{-\infty}^{\infty} W_\perp(\tau)\, e^{-i\omega\tau}\,\mathrm{d}\tau\,. \qquad (4)$$

The main contributors to the total impedance of the vacuum chamber are: finite conductivity of the walls (resistive-wall impedance), variations of the chamber cross section, high-order modes of accelerating RF cavities, electrostatic pickup-electrodes, strip-lines, flanges, bellows, synchrotron radiation ports, etc. If there is no interference of the wake fields excited by the beam in different components of the vacuum chamber (the components are far away from each other or the wake fields are rapidly damping), the impedances are additive at any frequency. In this case, the total impedance of the vacuum chamber can be represented as a sum of impedances of its components. For almost any component of a vacuum chamber, the impedance can be approximated by equivalent resonators with proper resonance frequencies, shunt resistances and quality factors. Since a narrowband oscillation mode is more long-living than the broadband mode, the beam interaction with the narrowband impedance and with the broadband one can be analyzed separately. We can assert that the narrowband impedance leads to the bunch-by-bunch interaction and can result in multi-bunch instabilities, whereas the broadband impedance leads to the intra-bunch interaction and can cause single-bunch instabilities. The beam stability is analyzed using the computed impedance or its simplified representation by resonators and resistive-wall impedance calculated analytically.

To compute the impedance of complex components of vacuum chambers, 3D finite-difference simulation codes [3, 4] are used. These codes solve Maxwell equations with the boundary conditions determined by the chamber geometry. The fields are excited by a bunched beam with pre-defined charge distribution, usually Gaussian. The simulation code

* Work supported by DOE under contract No.DE-AC02- 98CH10886.
† vsmalyuk@bnl.gov

ISBN 978-3-95450-187-8

output is a wake potential (3) which is a convolution of the wake function and the longitudinal bunch profile. Taking into account that the convolution of two time-domain functions is equivalent to the product of their Fourier transforms, the impedance is calculated as

$$Z(\omega) = \frac{\tilde{V}(\omega)}{\tilde{\lambda}(\omega)}\,, \tag{5}$$

where $\tilde{V}$ and $\tilde{\lambda}$ are the Fourier transforms of the wake potential and the longitudinal charge density, respectively. So the bandwidth of the impedance derived from the simulated wake potential is limited by the bunch spectrum width which is inversely proportional to the bunch length defined for the simulation. The mesh size of the solver is essential, it should be small enough to get reliable results for a given bunch spectrum. For a typical bunch length of few millimeters, full 3D simulation of wake fields in a big and complex structure is quite difficult because huge memory and processor time are required.

The beam-impedance interaction manifests itself in several effects of beam dynamics, some of these effects can be measured quite precisely using modern beam diagnostic instruments and measurement techniques.

LONGITUDINAL BROADBAND IMPEDANCE

For a beam-based measurement of longitudinal broadband impedance, we need to understand what can be measured. The measurable effects such as current-dependent bunch lengthening, synchronous phase shift, and energy spread growth due to microwave instability are dependent on integral parameters combining the impedance and the bunch spectrum. These parameters are the effective impedance and the loss factor. The normalized effective impedance $(Z_\parallel/n)_{\rm eff}$ is defined as

$$\left(\frac{Z_\parallel}{n}\right)_{\rm eff} = \frac{\sum\limits_{p=-\infty}^{\infty} Z_\parallel(\omega_p)\frac{\omega_0}{\omega_p} h_l(\omega_p)}{\sum\limits_{p=-\infty}^{\infty} h_l(\omega_p)}\,, \tag{6}$$

where $Z_\parallel(\omega)$ is the frequency-dependent longitudinal impedance, $n = \omega/\omega_0$ is the revolution harmonic number, $\omega_p = p\omega_0 + l\omega_s$, ω_0 is the revolution frequency, ω_s is the synchrotron frequency,

$$h_l(\omega) = (\omega\sigma_t)^{2l}\, e^{-\omega^2\sigma_t^2}\,, \tag{7}$$

is the spectral density of $l-$th Hermite mode (for a Gaussian bunch), $\sigma_t = \sigma_z/c$, σ_z is the bunch length. If the low-frequency longitudinal impedance is assumed as inductive, the normalized impedance $Z_\parallel/n$ is frequency-independent.

The coherent loss ΔE of the beam energy caused by the beam-impedance interaction is

$$\Delta E = k_\parallel q^2\,, \tag{8}$$

where q is the bunch charge, $k_\parallel$ is the loss factor

$$k_\parallel = \frac{\omega_0}{2\pi}\sum_{p=-\infty}^{\infty} Z_\parallel(\omega_p)h(\omega_p) = \frac{\omega_0}{\pi}\sum_{p=-\infty}^{\infty} \mathrm{Re}Z_\parallel(\omega_p)h(\omega_p)\,, \tag{9}$$

$h(\omega) = \tilde{\lambda}(\omega)\tilde{\lambda}^*(\omega)$ is the bunch power spectrum, $h(\omega) = e^{-\omega^2\sigma_t^2}$ for a Gaussian bunch. The second equality in (9) is valid because $\mathrm{Re}Z_\parallel(-\omega) = \mathrm{Re}Z_\parallel\omega)$ and $\mathrm{Im}Z_\parallel(-\omega) = -\mathrm{Im}Z_\parallel(\omega)$. If $\sigma_t\omega_0 \ll 1$, the sum can be replaced with the integral:

$$k_\parallel = \frac{1}{\pi}\int_{-\infty}^{\infty} \mathrm{Re}Z_\parallel(\omega)\, h(\omega)\mathrm{d}\omega\,. \tag{10}$$

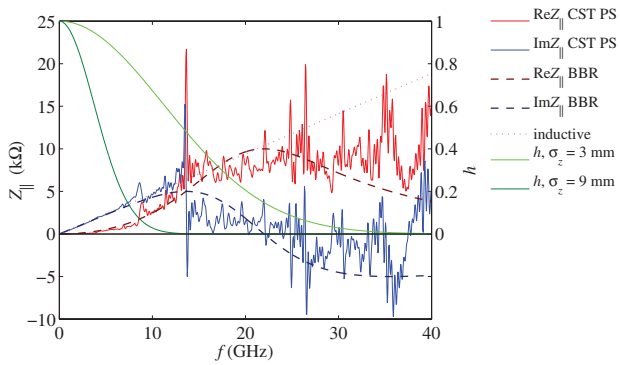

Figure 1: Longitudinal impedance and bunch spectra.

Figure 1 shows an example of the longitudinal impedance calculated by a 3D Maxwell equation solver CST Particle Studio together with a broadband resonator model and pure inductive impedance ($Z_\parallel/n = const$). The Gaussian bunch spectra are also shown for two bunch lengths: σ_z = 3 mm and σ_z = 9 mm. The measurable integral parameters, effective impedance and loss factor calculated using the simulated impedance and two simplified models are summarized in Table 1.

Table 1: Longitudinal Effective Impedance and Loss Factor

	σ_z = 3 mm		σ_z = 9 mm	
	$(Z_\parallel/n)_{\rm eff}$ Ω	$k_\parallel$ V/pC	$(Z_\parallel/n)_{\rm eff}$ Ω	$k_\parallel$ V/pC
Simulation	0.21	82	0.24	2.2
BBR	0.20	77	0.24	2.9
Inductive	0.25		0.25	

As one can see, the measurable single-bunch effects resulted from the beam interaction with a rather complex impedance such as the example shown in Figure 1 can be described with reasonable accuracy using a simple broadband resonator model. For longer bunches, even the simplest inductive model could be acceptable.

The reactive part of normalized effective impedance $\mathrm{Im}(Z_\parallel/n)_{\rm eff}$ can be estimated by measuring the r.m.s. bunch

ISBN 978-3-95450-187-8

length σ_t as a function of beam current I_b. The bunch length can be directly measured using a streak-camera, a dissector tube or, indirectly, by measuring the bunch spectrum width from a button-type pickup electrode. Interaction of a bunched beam with broadband impedance deforms the longitudinal bunch profile $\lambda(t)$, which is Gaussian for a zero-intensity bunch. At small beam currents, the energy spread of a relativistic electron beam is independent of its intensity and $\lambda(t)$ as a function of the average bunch current I_b can be described by the Haissinski integral equation [5]. The Haissinski equation can be solved numerically for a certain impedance model (i.e. broadband resonator) and the model parameters can be find by fitting the measured beam profile with the equation solution [6].

For a positive momentum compaction α, the intensity-dependent deformation of the longitudinal bunch profile $\lambda(t)$ causes the bunch lengthening, which can be approximately described by a cubic equation [7]:

$$\left(\frac{\sigma_t}{\sigma_{t0}}\right)^3 - \frac{\sigma_t}{\sigma_{t0}} = \frac{I_b\,\alpha}{\sqrt{2\pi}\,\nu_s^2\,(\omega_0\sigma_{t0})^3\,E/e}\,\mathrm{Im}\left(\frac{Z_\parallel}{n}\right)_{\mathrm{eff}} . \quad (11)$$

Formula (11) has been derived for the bunch lengthening of a relativistic electron or positron bunch caused by potential well distortion below the microwave instability threshold. The microwave instability results from the interaction between a large number of bunch oscillation modes growing and damping with their characteristic time constants. If the impedance can be considered as inductive, then to estimate the peak value of the threshold current I_p^{mwi}, the simple criterion [8] is applicable:

$$I_p^{\mathrm{mwi}} = \frac{\alpha\,E/e}{|Z_\parallel/n|}\left(\frac{\Delta p}{p}\right)^2_{\mathrm{FWHM}} , \quad (12)$$

where $\frac{\Delta p}{p} = \frac{\gamma^2}{\gamma^2-1}\frac{\Delta E}{E}$ is the momentum spread, which is equal to the energy spread $\Delta E/E$ for ultra-relativistic ($\gamma \gg 1$) beams.

The dynamics of longitudinal motion above the microwave instability threshold is characterized by the energy spread growth and a turbulent bunch lengthening with the beam current increase. The relative energy spread $\delta \equiv \sigma_E/E$ can be estimated from a measured transverse beam size which is determined by the combination of betatron and synchrotron contributions:

$$\sigma_x^2 = \beta_x\varepsilon_x + (\eta_x\delta)^2 , \quad (13)$$

where β_x is the beta function, ε_x is the transverse emittance, η_x is the dispersion. The transverse beam size is usually measured by a visible light monitor or a pin-hole X-ray camera located in a dispersive section.

Figure 2 shows an example of the measured bunch length (upper plot) and energy spread (lower plot) as functions of the beam current, the measurement was done at APS [9]. As one can see, it is practically impossible to find the microwave instability threshold from the bunch lengthening although

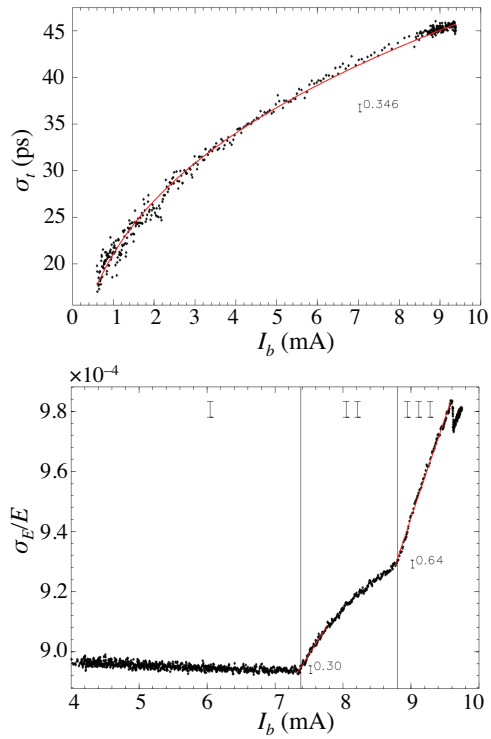

Figure 2: Measured bunch length (upper plot) and energy spread (lower plot) as functions of the beam current.

it is clearly visible on the energy spread graph, this is also confirmed by numerical simulations [10]. This means that formula (11) could be useful to fit the bunch lengthening even if the beam current exceeds the microwave instability threshold.

The coherent energy loss is compensated in the accelerating RF cavities every beam turn, as well as the energy loss caused by synchrotron radiation. The coherent energy loss leads to the current-dependent shift $\Delta\phi_s$ of the synchronous phase, which can be derived from the energy balance of the bunch:

$$\Delta\phi_s = \frac{I_b\,k_\parallel}{f_0 V_{\mathrm{RF}}\cos\phi_{s0}} , \quad (14)$$

where V_{RF} is the RF voltage, ϕ_{s0} is the synchronous phase at zero current. The phase shift is proportional to the beam current I_b and the loss factor $k_\parallel$, which in turn depends on the bunch length growing with the beam current, so the phase shift as a function of the beam current is non-linear. For small beam current, we can neglect the bunch lengthening and, with this approximation, the phase shift $\Delta\phi_s$ can be assumed proportional to the zero-current loss factor.

The current-dependent shift of synchronous phase can be measured directly using synchrotron light diagnostics (streak camera, dissector tube) or RF system diagnostics. To reduce the systematic error resulted from the drift or jitter of the diagnostic instruments, the two-bunch technique is useful. The longitudinal profiles of two bunches are measured simultaneously, one bunch has variable intensity, whereas

ISBN 978-3-95450-187-8

the other bunch with a fixed intensity is the reference. Figure 3 shows an example of two bunch profiles measured by a streak camera.

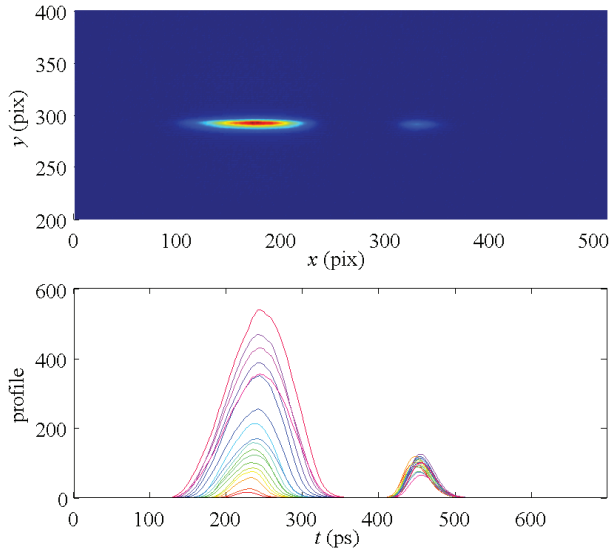

Figure 3: Reference bunch technique: bunch profile measured by a streak camera.

The other measurement technique is based on measuring the closed orbit deviation caused by the coherent energy loss [11]. If the dispersion and its derivation is zero in the accelerating RF cavities, the orbit deviation $x(s)$ can be assumed proportional to the dispersion $\eta(s)$:

$$x(s) \approx \eta(s)\delta_c(s) \, . \tag{15}$$

The relative energy loss per particle $\delta_c \equiv \Delta E/E$ is distributed along the ring as

$$\delta_c(s) = \frac{q}{E/e} \int_{s_{\mathrm{RFC}}}^{s} k'_{\parallel}(\zeta)\mathrm{d}\zeta \, , \tag{16}$$

and the orbit deviation caused by this energy loss, when the beam current $I_b = q f_0$ is changed by ΔI_b, is:

$$\Delta x(s) \approx \eta(s) \frac{\Delta I_b}{f_0 \, E/e} \int_{s_{\mathrm{RFC}}}^{s} k'_{\parallel}(\zeta)\mathrm{d}\zeta \, , \tag{17}$$

where $k'_{\parallel}$ is the specific loss factor per length unit of the beam orbit, s_{RFC} is the position of the accelerating RF cavity. The loss factor $k_{\parallel}$ can be estimated by measuring the closed orbit deviation as a function of the beam intensity [12]:

$$k_{\parallel} = \frac{f_0}{\Delta I_b} \frac{E}{e} \frac{\Delta x(s)}{\eta(s)} \, . \tag{18}$$

If the RF cavities are located in several places, this method can be used to measure the longitudinal loss factor of a section between the cavities. For every modern synchrotron, high-precision beam position monitors (BPMs) are now a standard component of beam diagnostics, so the beam orbit can be measured very precisely.

An example of the measured deviations of the horizontal and vertical orbits depending on the beam current is presented in Figure 4 [13]. Before the measurement, the orbit was corrected globally to minimize the influence of the transverse impedance. The intensity-dependent errors of the BPMs introduce a systematic error in the measurement results. We can assume that this error is of the same order for both horizontal and vertical planes. So, taking the vertical orbit deviation, which is less than 10% of the horizontal one (see Figure 4), and assuming zero dispersion in the vertical plane, we can conclude that the BPM-caused errors does not exceed 10%.

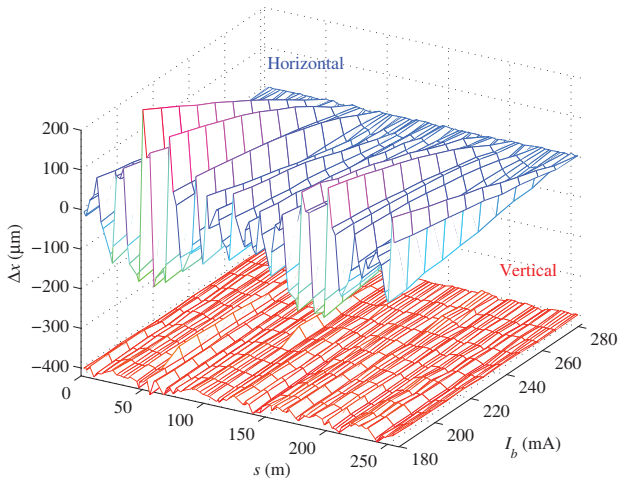

Figure 4: Orbit deviation as a function of beam current.

TRANSVERSE BROADBAND IMPEDANCE

For the transverse broadband impedance, the measurable effects are current-dependent shift of betatron tunes and rising/damping time of chromatic head-tail effect. Similar to the longitudinal impedance case, these effects are dependent on integral parameters combining the impedance and the bunch spectrum: transverse effective impedance and dipole kick factor. The transverse effective impedance $Z_{\perp\mathrm{eff}}$ is defined as

$$Z_{\perp\mathrm{eff}} = \frac{\sum_{p=-\infty}^{\infty} Z_{\perp}(\omega_p) h_l(\omega_p - \omega_\xi)}{\sum_{p=-\infty}^{\infty} h_l(\omega_p - -\omega_\xi)} \, , \tag{19}$$

where $Z_{\perp}(\omega)$ is the frequency-dependent transverse impedance, $\omega_p = p\omega_0 + \omega_\beta + l\omega_s$, $h_l(\omega)$ is the spectral density of l−th Hermite mode (7), $\omega_\xi = \xi\omega_0/\alpha$, $\xi = d\nu_\beta/(dE/E)$ is the chromaticity, $\omega_\beta = \nu_\beta\omega_0$ is the betatron frequency.

ISBN 978-3-95450-187-8

The transverse dipole kick $\Delta x'$ caused by the beam-impedance interaction is

$$\Delta x' = \frac{q}{E/e} k_\perp x \,, \tag{20}$$

where x is the beam transverse offset, $k_\perp$ is the dipole kick factor

$$k_\perp = \frac{\omega_0}{2\pi} \sum_{p=-\infty}^{\infty} Z_\perp(\omega_p) h(\omega_p) = \frac{\omega_0}{\pi} \sum_{p=-\infty}^{\infty} \mathrm{Im} Z_\perp(\omega_p) h(\omega_p) \,, \tag{21}$$

$h(\omega)$ is the bunch power spectrum. If $\sigma_t \omega_0 \ll 1$, the sum can be replaced with the integral:

$$k_\parallel = \frac{1}{\pi} \int_{-\infty}^{\infty} \mathrm{Im} Z_\perp(\omega)\, h(\omega) \mathrm{d}\omega \,. \tag{22}$$

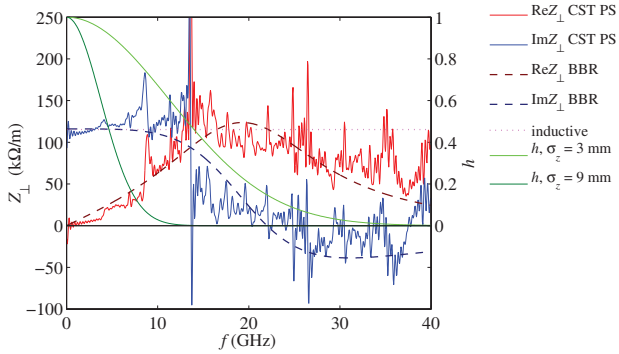

Figure 5: Transverse impedance and bunch spectra.

Figure 5 shows an example of the transverse impedance: result of wake field simulation, a broadband resonator model, and a pure inductive impedance ($Z_\perp = const$). The Gaussian bunch spectra are also shown for two bunch lengths: $\sigma_z = 3$ mm and $\sigma_z = 9$ mm. The measurable integral parameters, transverse effective impedance and dipole kick factor calculated using the simulated impedance and the simplified models are summarized in Table 2. As one can see, the measurable transverse single-bunch effects can be also described using the simplified models such as broadband resonator or pure inductive impedance for longer bunches.

Table 2: Transverse Effective Impedance and Kick Factor

	$\sigma_z = 3$ mm		$\sigma_z = 9$ mm	
	$Z_{\perp\mathrm{eff}}$ $k\Omega/m$	$k_\perp$ $V/(pC\,m)$	$Z_{\perp\mathrm{eff}}$ $k\Omega/m$	$k_\perp$ $V/(pC\,m)$
Simulation	101	2836	117	1083
BBR	97	2710	116	1075
Inductive	115		115	

Interaction of a bunched beam with short-range wake fields characterized by the broadband impedance, results in the transverse mode coupling. The wake fields induced by the bunch head act on particles of its tail part (a head-tail effect) and the head and tail of the bunch exchange places periodically due to synchrotron oscillations. If the chromaticity is zero, a fast head-tail instability occurs when the beam current exceeds a certain threshold. In the frequency domain, the instability threshold is reached when the coherent (center-of-mass) mode is coupled with the lowest (-1) head-tail mode. If the chromaticity is non-zero, a chromatic head-tail effect occurs. The coherent mode damps upon the positive chromaticity and becomes unstable when the latter is negative, and the higher-order head-tail modes behave oppositely. The rising/damping rates decrease rapidly with the mode number, and the higher-order modes are usually not dangerous for beam stability, since they are suppressed by the radiation damping. Since only a few of the lowest modes are essential, the eigenmode analysis is quite efficient for study of the head-tail effect. The complex frequency $\Omega = \omega + i/\tau$ of l-th head-tail mode can be found solving the eigenvalue problem [14]

$$\det\left[\left(\frac{\Omega - \omega_\beta}{\omega_s} - l\right)\mathbf{I} - \mathbf{M}\right] = 0 \,, \tag{23}$$

here ω_β is the unperturbed betatron frequency, τ is the rising/damping time, $\mathbf{I}$ is the unity matrix. The matrix elements are

$$M_{kk'} = I_b \frac{\beta}{2\nu_s E/e} \sum_{p=-\infty}^{\infty} Z_\perp(\omega_p) g_{lk}(\omega_p - \omega_\xi) g_{lk'}(\omega_p - \omega_\xi) \,, \tag{24}$$

where β is the average beta function. The functions g_{lk} characterizing oscillation modes of the Gaussian bunch are:

$$g_{lk}(\omega) = \frac{1}{\sqrt{2\pi k!(|l|+k)!}} \left(\frac{\omega\sigma_t}{\sqrt{2}}\right)^{|l|+2k} \exp\left(-\frac{\omega^2\sigma_t^2}{2}\right) \,. \tag{25}$$

If the frequency shift of coherent (0-th) mode is small compared with the synchrotron frequency ω_s, the linear approximation [14] is applicable:

$$\frac{d\Omega}{dI_b} = i \frac{\beta Z_\perp^{\mathrm{eff}}}{4\sqrt{\pi}\sigma_t E/e} \,. \tag{26}$$

If the chromaticity is positive, the frequency shift $\Delta\omega = \mathrm{Re}\Omega - \omega_\beta$ and chromatic damping time $\tau = 1/\mathrm{Im}\Omega$ of the coherent ($l = 0$) mode can be obtained by spectral analysis of beam oscillations registered by a turn-by-turn beam position monitor. Figure 6 shows the current-dependent shift of vertical betatron tune $\nu_y = \omega_y/\omega_0$ (upper plot) and damping rate $1/\tau_y$ (lower plot) [6]. The measured values are shown by blue points with errorbars, red lines represent the eigenvalues of (23) calculated for 3 values of chromaticity according to the measurements, the green lines represent the tracking results. The betatron tune graphs corresponding to different values of chromaticity are manually separated for better visibility.

ISBN 978-3-95450-187-8

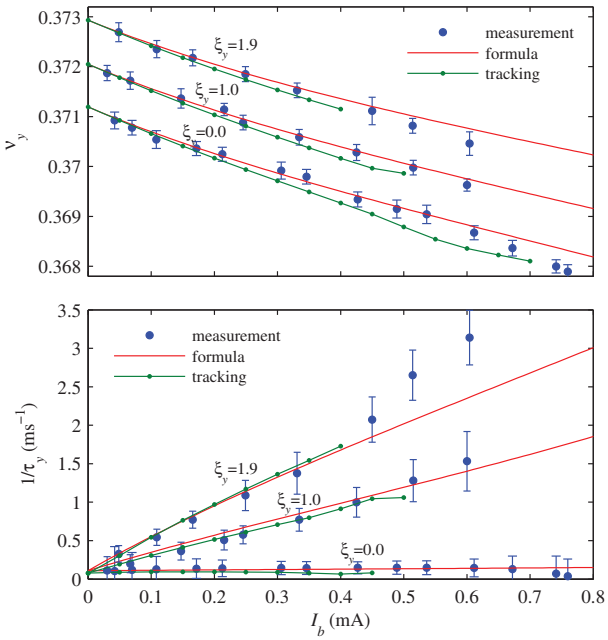

Figure 6: Vertical betatron tune ν_y (upper plot) and damping rate $1/\tau_y$ (lower plot) vs bunch current I_b. Measurement, formula and tracking.

LOCAL IMPEDANCE

Measurement of the betatron phase advance along the ring allows determining the contributions of different sections of the vacuum chamber into the coherent shift of betatron tune. In such a way, one can obtain the azimuthal distribution of the transverse impedance [12].

$$\Delta\mu(s) = -\frac{\Delta I_p}{8\pi CE/e}\int_0^s \beta(\zeta)\,\mathrm{Im}Z_\perp(\zeta)\,\mathrm{d}\zeta\,, \qquad (27)$$

where I_p is the peak bunch current ($I_p = \frac{\sqrt{2\pi}}{\omega_0\sigma_t} I_b$ for a Gaussian bunch), C is the ring circumference. Accuracy of this technique is determined by the single-turn resolution of the beam position monitors, the signals of which are used to calculate the betatron phase. A typical coherent betatron tune shift is of the order of 0.001 per 1 mA of the beam current and the BPM-to-BPM phase advance is much smaller, so this technique requires very good turn-by-turn resolution of BPMs.

The orbit bump technique [15, 16] is more sensitive because the BPMs are used in the narrowband orbit mode rather than in the broadband turn-by-turn mode and the noise is much smaller. This technique is based on the fact that an off-axis beam passing through the vacuum chamber section with a non-zero transverse impedance is deflected by the wake-fields. The beam-impedance interaction results in the transverse kick x' (20) proportional to the bunch charge q and its transverse position x at the location of the transverse impedance. If two closed orbits are measured with different beam intensity, the orbit deviation is:

$$\Delta x(s) = \frac{\Delta q}{E/e} k_\perp x_0 \frac{\sqrt{\beta(s)\beta(s_0)}}{2\sin\pi\nu}\cos\left(|\mu(s)-\mu(s_0)|-\pi\nu\right)\,, \qquad (28)$$

where x_0 is the orbit bump height, s_0 is the transverse impedance location, Δq is the bunch charge variation, ν is the betatron tune, β is the beta function, and μ is the betatron phase advance. This wave-like orbit deviation can be measured using beam position monitors, and the wave amplitude is proportional to the kick factor at the bump location. To reduce the systematic error caused by intensity-dependent behavior of the BPM electronics, this error is also measured and then subtracted. First of all, after the initial correction of the orbit to zero, two reference orbits x_{01} and x_{02} are measured at the high and low values of beam current. Then, after creating the orbit bump, again two orbits x_1 and x_2 are measured at the same beam current values. In the four-orbit combination $\Delta x = (x_2 - x_1) - (x_{02} - x_{01})$, the systematic error is eliminated, as well as the bump itself.

Rapid evolution of BPM electronics allows us to improve much the sensitivity of this technique. Now we can measure the orbit deviation of the order of several micrometers [17] compared to 100 micrometers orbit deviation measured at the very beginning of the bump method development [15], see examples in Figure 7.

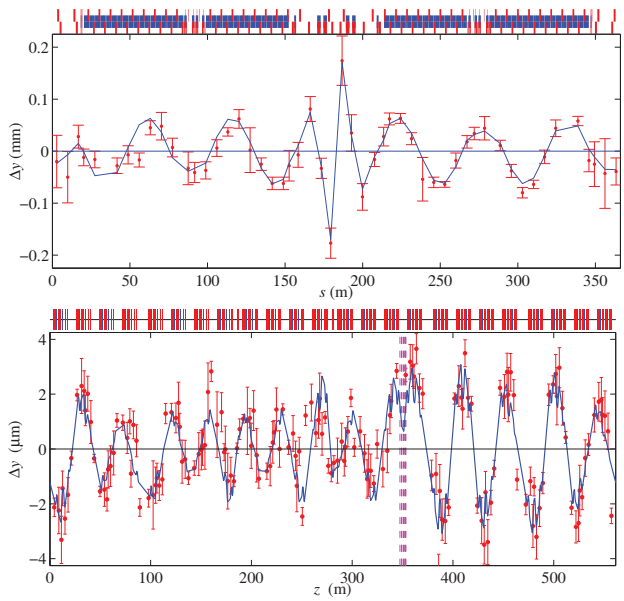

Figure 7: Measured orbit waves caused by a local impedance. Upper plot: VEPP-4M, 1998, lower plot: Diamond Light Source, 2014

To measure the impedance of a vacuum chamber component with variable geometry such as beam scrapers or in-vacuum undulators, both orbit and turn-by-turn techniques are effective. Using the reference bunch technique and high-precision BPMs, a contribution of the movable element to

ISBN 978-3-95450-187-8

the total shift of betatron frequency (26) can be measured quite accurately [18].

TRANSVERSE NARROWBAND IMPEDANCE

The motion of a multi-bunch train can be expanded in Fourier series, so we describe the motion in terms of multi-bunch modes. For a uniform fill pattern, if every RF bucket is occupied by a bunch with the same bunch current I_b, M bunches correspond to M modes, where M is the RF harmonic number. Without bunch-to-bunch interaction all bunches oscillate independently with the betatron frequency ω_β. Transverse multi-bunch instability is driven by long-range wake fields (narrowband impedance), usually trapped modes in cavity-like strictures in the vacuum chamber or resistive-wall impedance. If the bunches are coupled by the wake fields, each bunch oscillates with the frequency Ω, which becomes complex. For M bunches with finite length and internal modes, the complex frequency shift $\Delta\Omega = \Omega - \omega_\beta$ of the mode n is [14]:

$$\Delta\Omega_n = -\frac{i}{4\pi}\frac{\omega_0\beta}{E/e}MI_b\sum_{p=-\infty}^{\infty}Z_\perp(\omega_{pn})h_l(\omega_{pn}-\omega_\xi)\,, \quad (29)$$

where $\omega_{pn} = (pM+n)\omega_0 + \omega_\beta + l\omega_s$. The coherent frequency shift and growth rate are $\mathrm{Re}\Delta\Omega$ and $\mathrm{Im}\Delta\Omega$, respectively.

Almost all modern synchrotrons are equipped with transverse multi-bunch feedback systems (TMBF). These systems can be used as powerful beam diagnostic instruments. Using TMBF, we can excite the mode n by a stripline kicker driven at the frequency $\omega_{pn} = (pM+n)\omega_0 + \omega_\beta$, then stop the excitation and measure free oscillations (damped or anti-damped) and finally run the feedback to suppress any residual oscillation.

Figure 7 shows an example of vertical damping rates measured at Diamond light source [19]. The fit curve is calculated using formula (29). The resistive-wall impedance is calculated with the analytical formula

$$\frac{Z_y^{\mathrm{rw}}(\omega)}{L} = (\mathrm{sign}\omega + i)\frac{Z_0\delta_s(\omega)}{2\pi b^3}G_{1y}\,, \quad (30)$$

where $\delta_s(\omega)$ is the skin depth

$$\delta_s(\omega) = \sqrt{\frac{2c}{\mu_r\sigma_c Z_0|\omega|}}\,, \quad (31)$$

c is the speed of light, μ_r and σ_c are the relative permeability and conductivity of the chamber material, respectively; Z_0 is the free space impedance; b is the half-aperture, G_{1y} is the form-factor for an elliptical vacuum chamber [20]. The resonance peaks are fitted by narrowband resonators

$$Z_\perp^{\mathrm{res}}(\omega) = \frac{\omega_r}{\omega}\frac{R_s}{1+iQ\left(\frac{\omega}{\omega_r}-\frac{\omega_r}{\omega}\right)}\,, \quad (32)$$

where R_s is the shunt impedances, ω_r is the resonance frequency, and Q is the quality factor. Two of these resonances ("3" and "4" shown in Figure 8) can be attributed to the in-vacuum undulators. The effect of the undulator gaps closing was observed on the damping rates including both geometric impedance and contribution to the resistive wall impedance. Three other peaks ("1", "2", and "5") can be likely attributed to the beam position monitors (BPMs), this conclusion is based on comparison of the resonators fitting the measured data with the impedance obtained from wake field simulations.

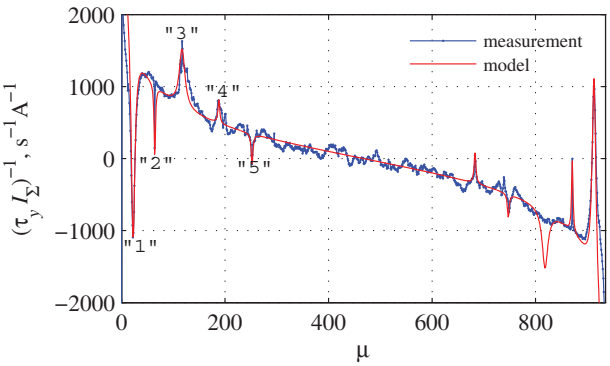

Figure 8: Vertical damping rates normalized by the beam current after subtraction of radiation damping (measured data in blue, fit in red).

CONCLUSION

Knowledge of impedances is necessary to understand collective effects of beam dynamics in accelerators. The most significant result of the collective effects is instability of longitudinal or transverse motion leading to deterioration of the beam quality or even to beam loss. Studies of collective effects are important both for designing new accelerators and for understanding the beam dynamics in the accelerators in operation. Calculation of impedance budget is an essential stage of a new accelerator design. There is a limited number of analytical formulae to calculate impedances of simplest vacuum chamber components but real vacuum chambers of modern accelerators usually have a complex geometry. Practically, finite-difference simulation codes are used for estimation of the impedance budgets. The problem is that the wake function is not calculated directly, the simulation code output is a wake potential which is a convolution of the wake function with longitudinal bunch profile. So the bandwidth of the impedance derived from the simulated wake potential is limited by the bunch spectrum width which is usually limited by computing capabilities. The impedance of an accelerator in operation can be studied experimentally using beam-based methods because the beam-impedance interaction manifests itself in various physical effects. The total frequency-dependent impedance is usually very complex so it is practically impossible to obtain its fine structure from the beam-based measurements. The measurable values

ISBN 978-3-95450-187-8

are integral parameters combining the impedance and the bunch spectrum, such as effective impedance, longitudinal loss factor or transverse kick factor. Using these measured parameters, simplified impedance models are usually developed to characterize and predict collective effects of beam dynamics.

REFERENCES

[1] B.W. Zotter and S.A. Kheifets, *Impedances and Wakes in High-Energy Particle Accelerators*, Singapore: World Scientific, 1998.

[2] W.K.H. Panofsky, W.A. Wenzel, *et al.*, "Some considerations concerning the transverse deflection of charged particles in radio-frequency fields", *Rev. Sci. Instrum.*, vol. 27, p. 967, 1956.

[3] W. Bruns, *The GdfidL Electromagnetic Field simulator*, `http://www.gdfidl.de/`

[4] Computer Simulation Technology, *CST Particle Studio*, `http://www.cst.com/Products/CSTPS`

[5] J. Haissinski, "Exact Longitudinal Equilibrium Distribution of Stored Electrons in the Presence of Self-Fields", *Nuovo Cimento*, vol. 18B, No. 1, 1973.

[6] V. Smaluk, I. Martin, R. Fielder, R. Bartolini, "Beam-based model of broadband impedance of the DIAMOND Light Source", *Phys. Rev. ST Accel. Beams*, Vol. 18, 064401 (2015).

[7] B. Zotter, "Potential-Well Bunch Lengthening", Rep. CERN SPS/81-14 (DI), Geneva, Switzerland, 1981.

[8] D. Boussard, "Observation of Microwave Longitudinal Instabilities in the SPS", Rep. CERN II/RF/Int.75-2, Geneva, 1975.

[9] Y.-C. Chae *et al.*, "Measurement of the Longitudinal Microwave Instability in the APS Storage Ring", in *Proc. PAC'01*, Chicago, USA, June 2001, paper TPPH068, pp. 1817-1819.

[10] A. Blednykh *et al.*, "A Numerical Study of the Microwave Instability at APS", in *Proc. NA-PAC'2016*, Chicago, October 2016, paper TUPOB51.

[11] J.P. Koutchouk, "Trajectory and closed orbit correction", Rep. CERN LEP-TH/89-2, Geneva, Switzerland, 1989.

[12] D. Brandt *et al.*, "Measurement of Impedance Distribution and Instability Threshold in LEP", in *Proc. PAC'95*, Dallas, Texas, USA, May 1995, paper RAA20, pp. 570-572.

[13] E. Karantzoulis, V. Smaluk, L. Tosi, "Broad Band Impedance Measurements on the Electron Storage Ring ELETTRA", *Phys. Rev. ST Accel. Beams*, Vol. 6, 030703 (2003).

[14] A. Chao, *Physics of Collective Beam Instabilities*, Wiley, New York, 1993.

[15] V. Kiselev, V. Smaluk, "Experimental Study of Impedances and Instabilities at the VEPP-4M Storage Ring", in *Proc. EPAC'98*, Stockholm, Sweden, June 1998, paper THP09F, pp. 1005-1007.

[16] V. Kiselev, V. Smaluk, "Measurement of Local Impedance by an Orbit Bump Method", *Nucl. Instr. and Meth*, A 525 (2004).

[17] V. Smaluk *et al.*, "Coupling impedance of an in- vacuum undulator: Measurement, simulation, and analytical estimation", *Phys. Rev. ST Accel. Beams*, Vol. 17, 074402 (2014).

[18] B. Podobedov *et al.*, "Novel Accelerator Physics Measurements Enabled by NSLS-II RF BPM Receivers", in *Proc. IBIC2016*, Barcelona, Spain, 2016, paper TUCL02.

[19] R. Bartolini *et al.*, "Analysis of Multi-bunch Instabilities at the Diamond Storage Ring", in *Proc. IPAC'16*, Busan, Korea, May 2016, paper TUPOR013, pp. 1685-1687.

[20] R.L. Gluckstern, J. van Zeijts, B. Zotter, "Coupling Impedance of Beam Pipes of General Cross Section", *Phys. Rev.*, E vol. 47 No. 1, 1993.

ISBN 978-3-95450-187-8